Study of the intermediate state in MnF_2 by means of antiferromagnetic resonance and the Faraday effect

V. V. Eremenko, A. V. Klochko, and V. M. Naumenko

Physicotechnical Institute of Low Temperatures, Academy of Sciences of the Ukrainian SSR
(Submitted 18 March 1985)
Zh. Eksp. Teor. Fiz. **89**, 1002–1017 (September 1985)

It is demonstrated experimentally that the internal magnetic field in an antiferromagnet in the intermediate state is uniform and constant. The oscillations in the domains of the antiferromagnetic and spin-flop phases occur independently of each other. The field region in which the coherent intermediate state occurs is the region in which the antiferromagnetic resonance frequencies are independent of the external magnetic field and the Faraday rotation angle changes linearly with the field.

1. INTRODUCTION

When certain antiferromagnets are placed in an external magnetic field whose direction coincides with the spontaneous direction of the antiferromagnetism vector, a first-order orientational phase transition—the tipping of the magnetic sublattices (spin-flop transition)—occurs when the field reaches a critical value. In a sample of finite dimensions this transition occurs through an intermediate state (IS),[1,2] which is a thermodynamically stable regular structure consisting of domains of the antiferromagnetic (AF) and spin-flop (SF) phases separated by thin domain walls. The field interval in which the intermediate state exists, ΔH_{IS}, is determined by the demagnetizing field $\mathbf{H}_M$ of the sample:

$$\Delta H_{IS} = |\mathbf{H}_M| = 4\pi N_z M_z,$$

where M_z is the z component of the magnetization of the sample in the SF phase, and N_z is the demagnetizing factor along the spontaneous direction of the antiferromagnetism vector (the z axis).

The first experimental proof[2] of the existence of the intermediate state in an antiferromagnet was obtained in a study of the magnetization of the tetragonal two-sublattice antiferromagnet MnF_2. That study[2] measured such parameters of the intermediate state as the critical angle ψ_{cr} and ΔH_{IS}. The critical angle for a cubic sample was 30′, and the field for which the intermediate state exists varied with sample shape from 0.04 T for a cylinder to 0.09 T for a thin disk. The intermediate state in this crystal was subsequently studied by means of optical spectroscopy[3,4] and nuclear magnetic resonance.[4] King and Paquette[4] made visual observations of the domain structure, which turned out to be quite regular and had an average period of 84 μm; the evolution of this domain structure with changing magnetic field was found to agree with the theory and with general physical considerations. Antiferromagnetic resonance (AFMR) studies should also yield much important information on the intermediate state. The AFMR should exhibit unusual behavior characteristic of the intermediate state. The signs of such behavior can be found by recognizing that as the external magnetic field changes, the internal magnetic field in an antiferromagnet in the intermediate state remains constant and uniform. Also taking into account the fact that the coupling between the oscillations in the AF and SF domains cannot be strong in view of the small value of the susceptibility of the antiferromagnet, one would expect that the AFMR frequencies in the intermediate-state region will remain practically unchanged when the external magnetic field changes. The oscillations in the AF and SF phases should occur independently of each other, and their intensities should be proportional to the fraction of the material that is in the corresponding phase. In the intermediate state of $CuCl_2 \cdot 2H_2O$, however, the AFMR frequency was found[5] to vary smoothly with increasing field; this was interpreted as the observation of a superposition of the oscillations of the magnetic moments in the AF and SF domains. Therefore, it has become necessary to do a careful and convincing experiment on an object whose intermediate state has been rather well studied by other methods. For this reason we have chosen to study manganese fluoride, which, moreover, has a simple magnetic structure, permitting unambiguous interpretation of the experimental results and the use of the conclusions of the existing theory of the intermediate state.[1] In particular, it is fortunate that the fourth-order anisotropy constant in this crystal is small. A significant value of this constant greatly complicates the orientational phase transition,[6,7] and there is no corresponding theoretical analysis of the intermediate state.

A study of the AFMR in the intermediate state is not only of interest in its own right; a systematic study permits identification of the order of the transition, determination of the critical angle and the boundaries of the intermediate state, etc. In this regard it is useful to compare the experimental data obtained under identical conditions in AFMR, magnetic susceptibility, and Faraday effect studies near the resonance frequencies. The Faraday effect, as we know, depends on the magnetization and should therefore be very sensitive to the features of the intermediate state. A brief report of this study was published earlier.[8]

2. EXPERIMENTAL TECHNIQUES AND SAMPLES

The experiment was done on a cavityless spectrometer of the transmission type,[9] permitting investigation of the

 0038-5646/85/090576-10$04.00

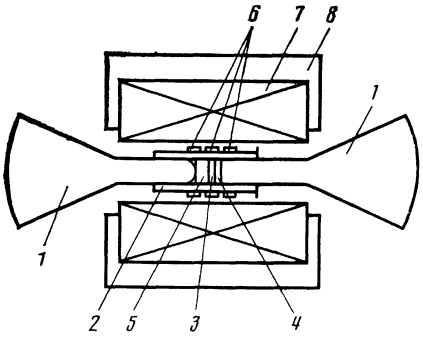

FIG. 1. Measurement cell with solenoid: 1) conical lenses, 2) sleeve, 3) sample, 4) polyethylene disk containing DPPH, 5) plane-parallel plate, 6) measurement coils, 7) solenoid, 8) steel belt.

wavelength region 0.3–7 mm (33 cm^{-1}–1.45 cm^{-1}) in a pulsed magnetic field up to 30 T. The radiation sources were backward wave tubes, and the receiver was an n-InSb crystal cooled to 4.2 K. The stability of the wavelength of the tube depended mainly on the stability of the voltage across its slow-wave system and amounted to 10^{-4}. By measuring this voltage with a digital voltmeter, we could rapidly determine the wavelength to high accuracy from a calibration curve taken earlier.

The sample was placed at the center of a solenoid and clamped by two conical lenses (1) which went over to dielectric waveguides of square cross section inserted into a sleeve (2) (Fig. 1). Mounted between the waveguides were the sample (3), a polyethylene disk (4) containing a small quantity of α-diphenyl-β-picryl hydrazyl (DPPH) for calibrating the field, and a plane-parallel Teflon plate (5). To avoid warping and cracking of the sample, the right-hand conical lens was inserted tightly into the sleeve, while the left-hand lens had a rounded end and was inserted freely, with a small gap, into the sleeve, precompressing plate (5). Then the mechanical load was uniformly distributed over the plane of the sample. The sleeve was wound with a coil (6) for measuring the field and susceptibility.

By recording the longitudinal differential magnetic susceptibility $\chi_z = dM_z/dH$ (z coincides with the tetragonal axis C_4) on the oscilloscope screen simultaneously with the resonance absorption curves of the electromagnetic radiation we could track the magnetic state of the antiferromagnet and its orientation in the external magnetic field and compare the static and dynamic properties. This technique also gave a good field calibration point, corresponding to the maximum of χ_z, with respect to which the resonance field in the intermediate-state region could be measured with an accuracy of $5 \cdot 10^{-3}$ T. This was done in the following way. We were mainly interested in the magnetic-field region near the field of the SF transition (i.e., around 0.5 T). Therefore, for the purpose of observing the features of the intermediate state we inserted into the sweep trigger of the oscilloscope a precision delay with respect to the beginning of the magnetic-field pulse and chose the sweep rate in such a way that the field region under study filled the entire horizontal dimension of the oscilloscope screen. In this case the change in the field during the sweep time of the oscilloscope beam could be considered proportional to the time, and the field intervals could be measured by simply measuring the distance to the χ_z peak. The coefficient of proportionality was determined from the marker DPPH on changes in the frequency of the backward wave tube; this frequency was measured by a wavemeter to high accuracy. In order for this coefficient of proportionality to remain constant from one magnetic-field pulse to another, it was necessary to have the same value of the initial voltage across the capacitor bank feeding the solenoid. The stability of the apparatus maintaining the voltage across the bank and the stability of the delay were such that the position of the χ_z peak from one pulse to another did not change with respect to the marks on the oscilloscope screen.

Absolute calibration of the magnetic susceptibility signal of MnF_2 with respect to the magnetic field was achieved with the aid of the marker DPPH at a frequency of 8.59 cm^{-1}, permitting determination of the value of the spin-flop transition field to an accuracy of 10^{-2} T. The nonuniformity of the field at the location of the sample was not more than 0.1% of its absolute value.

As the source of the pulsed magnetic field was mainly used a solenoid, giving an experimental geometry of $\mathbf{h}_\omega \perp \mathbf{H} \| C_4$, here $\mathbf{h}_\omega$ is the vector of the rf radiation incident on the sample. In the intermediate state, however, resonance absorption could also be expected for $\mathbf{h}_\omega \| \mathbf{H} \| C_4$. To do the latter experiment we used a Helmholtz coil. The rise time of the magnetic field from zero to its maximum value was $2.5 \cdot 10^{-3}$ sec, while its rate of change in the region of the intermediate state was $2.9 \cdot 10^{-3}$ T/μsec, the usual value for studies in pulsed magnetic fields.[2,3] Of particular importance is the accuracy of the orientation of the tetragonal axis of the sample with respect to the external magnetic field $\mathbf{H}$ and the reliability of the monitoring of this orientation, since the critical angle in MnF_2 is small and, moreover, in the process of the measurements it is necessary to give calibrated angles of inclination. These requirements were met by a zero-free-play rotating device of our own design,[9] which permitted us to vary the orientation of the sample with respect to the solenoid in two planes with an accuracy of $\pm 30''$. In repeated cycles involving heating and cooling of the solenoid and rotating device, the orientation of the sample in the solenoid channel was maintained. The solenoid and sample are immersed in a liquid coolant. High-quality samples were required for the experiments. The quality control was carried out visually from the conoscope figures and Laue patterns, which were also used to determine the crystallographic directions [100] and [001] (i.e., the C_2 and C_4 axes).

For the study with the solenoid under the condition $\mathbf{k} \| \mathbf{H}$ ($\mathbf{k}$ is the wave vector), we cut square plates 3.5 mm on a side, with the cuts along the [100] and [010] directions. Here the plane of the plate was perpendicular to the C_4 axis to an accuracy of 30′ or better, which is necessary for decreasing the influence of the additional components of the demagnetizing field on the parameters of the intermediate state. The thickness of the plate was varied over the range 0.07–1.5 mm. For the experiments with the Helmholtz coil we used square plates 3.2 mm on a side and 0.4 mm thick; the C_4 axis was parallel to one of the sides of the square, and the C_2 axis to the other side. The samples were carefully pol-

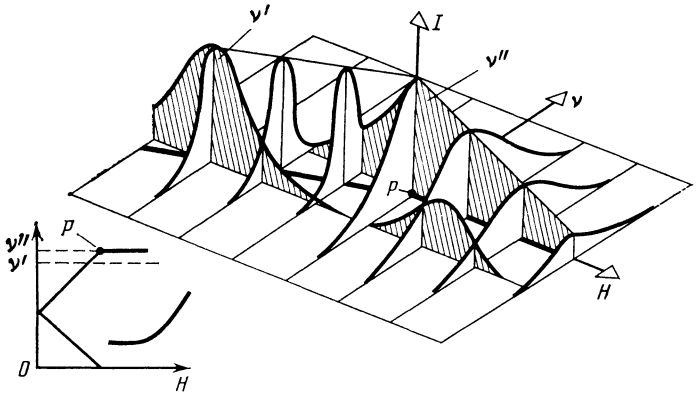

FIG. 2. Method of reconstructing resonance lines $I(\nu,H_j = \text{const})$ for a frequency sweep from the experimental data obtained in a field sweep of the spectrum $I(H,\nu_j = \text{const})$ (schematic). To avoid excessive complication of the diagram, this illustration uses only two initial contours $I(H,\nu_j = \text{const})$, corresponding to the frequencies ν' and ν'' on the frequency-field curve shown in the inset.

ished. For observation of the high-frequency mode of the AFMR in the intermediate state the optimum sample thickness was about 0.07 mm, so that the absorption lines were intense. A sample of such a thickness can be prepared only by cementing it to a substrate. This led to broadening of the absorption lines and to a small distortion of the frequency-field curve. To observe the SF mode in the intermediate state in such a sample is very difficult, since the intensity of the corresponding lines is much weaker than for the high-frequency mode. Here it was necessary to use a sample about 0.3 mm thick. It was desirable to study the behavior of the AF and SF modes in the same sample, so the measurements were mainly taken on samples about 0.3 mm thick and, although the lines of the high-frequency mode were somewhat saturated, this had practically no effect on the main experimental results. The samples were oriented to within $\pm 10'$ by the position of the χ_z peak, and, more accurately, by the appearance of absorption at as high a frequency as possible for the high-frequency mode of the AFMR and the absence of absorption at lower frequencies. Such an orientation also corresponded to the appearance of absorption at the lowest frequency for the SF mode in the intermediate state. The accuracy of this method of aligning the samples was $\pm 30''$.

As we mentioned in the Introduction, the AFMR frequencies in the intermediate-state region were expected to be independent of the strength of the magnetic field; this situation would be expressed in the presence of horizontal regions on the $\nu(H)$ curve. These horizontal regions are easily observed by sweeping the spectrum $I = I(H_j,\nu)$ over frequency at fixed values of the external field H_j (here I is the intensity of the radiation transmitted through the sample). Although backward wave tubes do not permit a frequency sweep of the spectrum, the finite width of the resonance lines makes it possible to successfully study the horizontal regions on the frequency-field curves even in the usual experimental situation where one can only sweep in field, $I = I(H,\nu_j)$. For this purpose it is necessary to record the spectrum $I(H,\nu_j)$ at frequencies ν_j differing from one another by substantially less than a linewidth, making it possible to reconstruct the shape of the absorption lines $I(\nu,H_j)$ if one has a sufficiently complete set of spectra $I(H,\nu_j)$. To reconstruct the profile of the absorption line $I(\nu,H_j)$ on a three-dimensional coordinate grid $I(\nu,H)$, one must plot the experimental profiles of the absorption lines $I(H,\nu_j)$ (the hatched profiles in Fig. 2). The resulting ensemble of profiles is cut by planes perpendicular to the H axis. The points of intersection of these planes with the contours $I(H,\nu_j)$ are connected by smooth curves, giving the profiles $I(\nu,H_j)$. The lines drawn through the projections of the tops of the $I(\nu,H_j)$ profiles onto the (ν,H) plane are the frequency-field curves taken in the frequency cross section, and can reflect the constancy of the AFMR frequency in the intermediate state.

For measuring the changes in the Faraday rotation angle at the SF transition an analyzer was mounted between the receiver and the cryostat containing the sample; the analyzer was a grating of parallel wires with a period of 50 μm (the diameter of the wires was 20 μm). The analyzer was turned to an angle of 45° with respect to the position at which the transmission of the electromagnetic wave was a minimum. In this case, as we know, the change in the Faraday rotation angle is proportional to the change in the intensity of the transmitted electromagnetic radiation at Faraday rotation angles much smaller than $\pi/4$.

3. EXPERIMENTAL RESULTS

The frequency-field curve of the AFMR in MnF_2 at a temperature of 4.2 K in the case when the magnetic field is oriented precisely along the tetragonal axis of the crystal is shown in Fig. 3. The experimental points outside the intermediate-state region conform well to the theoretical

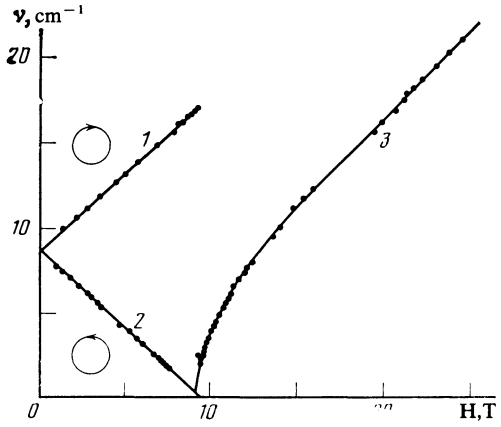

FIG. 3. Frequency-field curve of AFMR in MnF_2 for $\psi = 0 \pm 0.5'$; numbers 1, 2, and 3 denote the high-frequency, low-frequency, and spin-flop modes, respectively. The circles with arrows indicate the polarization of the absorption lines. The solid curves are theoretical.[11,19]

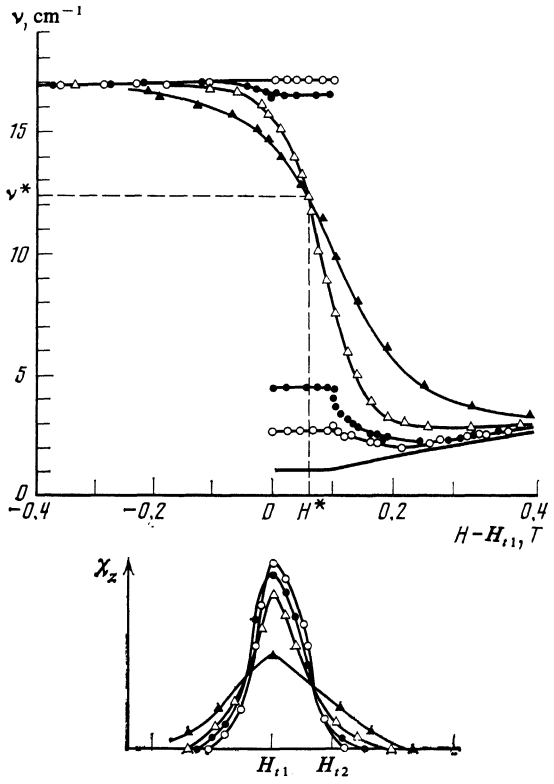

FIG. 4. Frequency-field curve of AFMR and the static susceptibility χ_z for various angles of inclination ψ: ○) $0 \pm 0.5'$; ●) 10'; △) 20'; ▲) 40'; ν^* and H^* are the coordinates of the point of intersection of the frequency-field curves; H_{t1} and H_{t2} are the boundaries of the horizontal regions on the frequency-field curves for $\psi = 0$. The solid curve at the bottom is the theoretical curve[11,19] for $\psi = 0$.

curves[10,11] for $g = 2.00$. In the intermediate-state region there is no absorption in the frequency interval 3.5–16.5 cm^{-1}. For $\psi \neq 0$ (ψ is the angle of inclination of the field relative to the tetragonal axis of the crystal) the "window" of transparency decreases in size, vanishing at $\psi = \psi_{cr}$; this can be seen from Fig. 4, which shows the frequency-field curves in expanded scale near the intermediate-state region for different angles ψ. The lower part of Fig. 4 shows the magnetic-field curves of the susceptibility $\chi_z(H)$ for various angles ψ. We can see horizontal regions, corresponding to the intermediate state, on the frequency-field curves for angles $\psi < \psi_{cr}$. With increasing angle of inclination of the field the horizontal regions on the frequency-field curves decrease in size, and when the angle of inclination reaches its critical value ψ_{cr} these regions contract into a point, with coordinates $\nu^* = 12.4 \pm 0.2\ cm^{-1}$ and $H^* = 9.26 \pm 0.01$ T. At this point the frequency-field curves for all angles of inclination greater than ψ_{cr} intersect. The location of the point (ν^*,H^*) was determined experimentally by finding a frequency of the backward wave tubes such that the absorption line in the region of the SF transition did not shift with increasing angle of inclination after the value ψ_{cr} was reached.

The experimental points on the horizontal parts of the frequency-field curves were obtained by the technique described in Sec. 2, which amounts to the replotting of the $I(H,\nu_j)$ into $I(\nu,H_j)$ contours. The result of this replotting is shown in Fig. 5, which illustrates several $I(\nu,H_j)$ contours which reflect the absorption of the high-frequency mode of the AFMR at various values of the external magnetic field H_j. Each of these contours is constructed from 18 spectrograms $I(H,\nu_j = \text{const})$ taken with a frequency step of about 0.03 cm^{-1}.

The scatter of the points describing the $I(\nu,H_j = \text{const})$ contours amounts to about 10% for the maximum and 20–30% for the wings; this gives a scatter of ± 0.025 cm^{-1} in the frequency positions of the lines. We see from Fig. 5 that the contour corresponding to a field of 8.97 T differs from the others. Its shape is nearly Lorentzian, and its width at half-height, 0.15 cm^{-1}, is noticeably narrower than that of the other contours. This contour lies outside the limits of the SF transition and corresponds to the "pure" AFMR line. The contours corresponding to fields 9.05 and 9.12 T have a width of 0.3 cm^{-1} and are becoming asymmetric. The asymmetry is evidently due to the imperfect orientation of the sample and to slight imperfections in the sample itself. These contours already "feel" the SF transition; they correspond to the leading edge of the susceptibility signal $\chi_z(H)$ when the SF transition has begun in a small part of the sample on account of defects in the sample and nonuniformity of the internal field. The nonuniformity of the internal field is due to the nonuniformity of the external magnetic field and to the nonellipsoidal shape of the sample. The main defect in the sample is evidently the presence of blocks having a slight relative misalignment of their antiferromagnetism vectors **l**. On further growth in the field on the segment

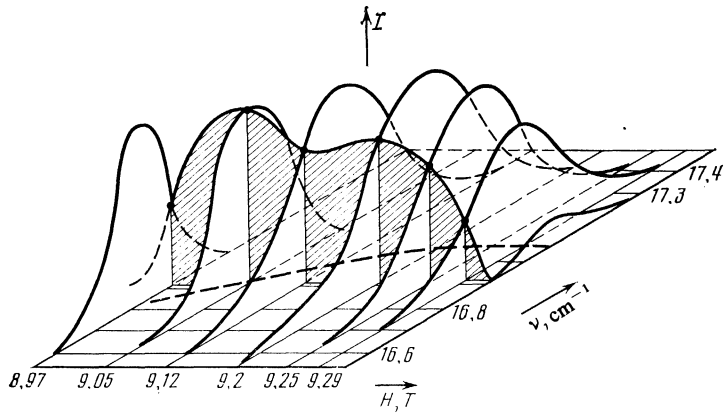

FIG. 5. Contours of the resonance absorption lines of the high-frequency mode of the AFMR reconstructed for $I = I(\nu,H_j = \text{const})$ from the oscilloscope traces of $I = I(H,\nu_j = \text{const})$. For illustration of the method of construction we have taken only one of the initial contours $I = I(H,\nu_j = 16.92\ cm^{-1})$. The heavy dashed line is the frequency-field curve.

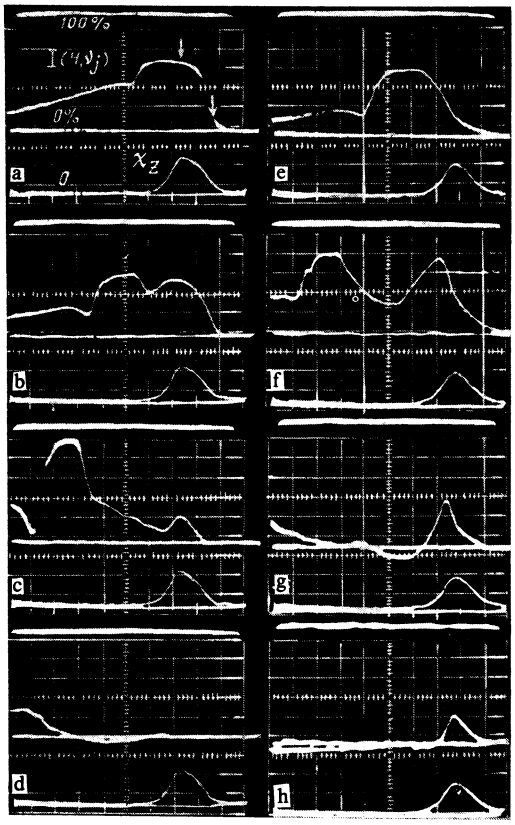

FIG. 6. Oscilloscope trace of $I(H,\nu_j = \text{const})$ for the high-frequency mode and $\chi_z(H)$ for the region of the spin-flop transition; left (a–d) $\psi = 0$, right (e–h) $\psi = 10'$; a) ν [cm^{-1}] = 17.14; b) 16.92; c) 16.75; d) 16.66; e) 17; f) 16.8; g) 16.52; h) 15.9. The arrows on trace *a* indicate the beginning (H_{t1}) and end (H_{t2}) of the intermediate state.

corresponding to the trailing edge of the $\chi_z(H)$ signal and to the residence of the sample in the intermediate state, the width of the lines increases somewhat further, and their intensity falls off in accordance with the decrease in the overall fraction occupied by the AF phase. It should be noted that in the field interval 9.05–9.2 T the integrated intensity of the lines increases somewhat, but this should not be considered significant since, for the reasons discussed above, the sample thickness was chosen somewhat larger than the optimum.

Figure 6 shows illustrative oscilloscope traces of the high-frequency mode for $\psi = 0$ (left) and $\psi = 10'$ (right), by which we can follow the evolution of the lines. Each of the traces has 3 horizontal lines, corresponding to the zero level of χ_z and to the zero and 100% absorption levels for the microwave radiation; the lower trace is $\chi_z(H)$. Trace *a* corresponds approximately to the cross section along the horizontal part of the frequency-field curve. We see the pure AFMR line, going over to the line corresponding to the intermediate state. The gently sloping wing of the line is formed partly by the uncontrolled influence of the Faraday rotation and partly by interference effects. The Faraday rotation affects the shape of the lines because of the polarization properties of the beam channel of the spectrometer between the sample and the receiver and also because of the polarization properties of the sample due to its square cut.

For these same reasons the intensity of the line at the maximum exceeds 50%, which should not happen in view of the fact that the microwave radiation is linearly polarized and the normal wave for the excitation of the AFMR is circularly polarized. In the field region corresponding to the intermediate state, the intensity of the line of the high-frequency mode of the AFMR should decrease linearly with increasing field, but because of saturation of the lines this does not occur. As soon as the line leaves the saturation region the expected linear dependence appears (traces c and e–h). Trace b corresponds to a lower frequency of the backward wave tube. We see that the pure AFMR line is shifted to lower fields. Trace c corresponds to a cross section on the "tail" of the AFMR line in the intermediate state (in lower fields we see the saturated AFMR line in the AF state), and trace d corresponds to the transparency window. We see from these traces that the beginning and end of the intermediate-state region can be detected from the beginning and end of the linear dependence of the intensity without recourse to construction of the frequency-field curves. This can be done in an analogous way from the intensity curve for the absorption line of the SF mode, a trace of which is shown in Fig. 7 (in the cross section along the lower horizontal part of the frequency-field curve of Fig. 4). On the left in the trace is the line of the SF mode of the AFMR in the intermediate-state region; this line goes over to the line of the SF mode outside the limits of the SF transition. The beginning of the intermediate-state region (the transition field H_{t1} from the AF state to the intermediate state) corresponds to the appearance of the SF mode, while the end of the intermediate-state region (the transition field H_{t2} from the intermediate state to the SF state) is more clearly seen from the traces for the high-frequency mode of the AFMR. The width of the intermediate-state region determined in this way is 0.1 T, in good agreement with the estimate $\Delta H_{IS} = H_{t2} - H_{t1} = 4\pi N_z M_z$ [$N_z = 0.8$ for a sample of the given shape, and $M_z = 9.8 \cdot 10^{-3}$T (Ref. 2)]. Thus we observe a decrease in

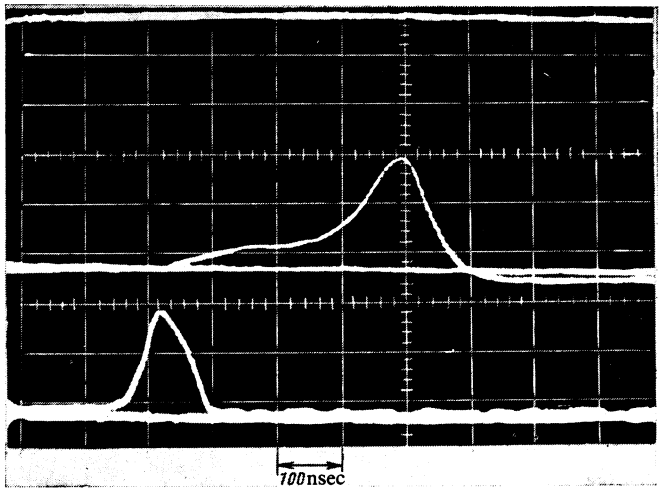

FIG. 7. Oscilloscope trace of $I(H,\nu_j = 2.5\ \text{cm}^{-1})$. The spin-flop mode in the cross section along the horizontal part of the frequency-field curve for $\psi = 0$. The lower trace is $\chi_z(H)$.

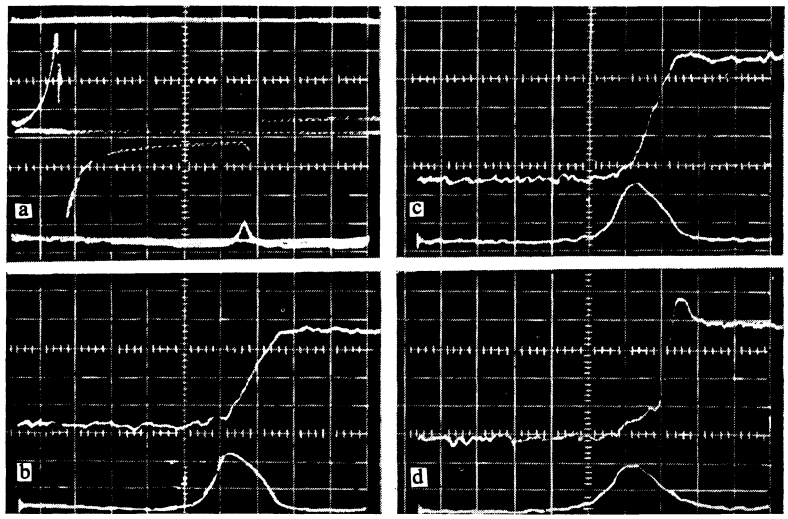

FIG. 8. Faraday rotation angle as a function of the strength of the magnetic field for various ψ: a) 1°12′; b) 0; c) 10′, d) 19′; $\nu = 11.4$ cm^{-1}. The lower traces are $\chi_z(H)$.

the intensity of the AFMR line of the high-frequency mode and an increase in the intensity of the SF mode as the external field increases from H_{t1} to H_{t2}; here the regions in which oscillations of the two modes exist overlap in field. It is possible that oscillations are excited at the frequency 2.5 or 17.1 cm^{-1} of one of the horizontal regions of the frequency-field curve for a strict orientation of the field along the C_4 axis, but not at the intermediate frequency.

Although for $\psi = 0$ there is no absorption in the frequency interval 3.5–16 cm^{-1}, this region is optically active, since the sign of the Faraday rotation changes at the SF transition, as can be seen from the oscilloscope traces in Fig. 8, which were taken with the analyzer in place. In trace 8a the field increases from 0 to 10.6 T, and the angle of inclination of the magnetic field with respect to the tetragonal axis of the crystal is 1°12′. The overshoots seen on this trace are due to the rotation of the polarization in the wings of the absorption lines. Trace b ($\psi = 0$) exhibits no overshoots corresponding to the absorption line of the SF mode, and the Faraday rotation angle changes linearly in the field interval H_{t1}–H_{t2} (in traces b–d the horizontal scale is expanded 10 times and the vertical scale 5 times). Faraday rotation can determine the width of the intermediate-state region more accurately, since both boundaries of the intermediate state are clearly visible on the same frame. According to the Faraday rotation data, $\Delta H_{IS} = (0.1 \pm 0.005)$ T. As the angle of inclination of the magnetic field with respect to the C_4 axis increases, the linear region of the Faraday rotation narrows (trace c), and when the angle ψ_{cr} is reached (trace d) an overshoot to larger fields appears if $\nu < \nu^*$ or to smaller fields if $\nu > \nu^*$; this is indicative of the proximity of the absorption line. The critical angle ψ_{cr} determined by the Faraday rotation is $18 \pm 1'$.

It should be noted that for $\psi = 0$ the intensity of the absorption in the intermediate-state region at a frequency of 2.5 cm^{-1} is approximately one-fifth as large as the intensity of the line of the SF mode at this same frequency but outside the intermediate-state region (Fig. 7). A similarly weak intensity is found for the line corresponding to the SF mode on the region of the frequency-field curve with a negative derivative dv/dH at $\psi = 0$ (Fig. 4). This ratio of the intensities of the absorption lines is not seen for the high-frequency mode of the AFMR at a frequency of 17.1 cm^{-1} (Fig. 6a). We have not found an explanation for this fact.

Finally, we note that in the experiments with $\mathbf{h}_\omega \| \mathbf{H} \| C_4$ we observed no absorption in a window of transparency from 3.5 to 16.5 cm^{-1} when the external magnetic field was oriented strictly along the C_4 axis.

4. THEORY

The density of the homogeneous magnetic energy of a uniaxial antiferromagnet, including the energy of the demagnetizing field, is of the form[12]

$$\mathcal{H} = \delta \mathbf{M}_1 \mathbf{M}_2 - (\rho/2)(M_{1z}^2 + M_{2z}^2) - \mathbf{HM} + 2\pi \mathbf{M} \hat{N} \mathbf{M}, \qquad (1)$$

where δ and ρ are the exchange and anisotropy constants, $\mathbf{M}_1$ and $\mathbf{M}_2$ are the sublattice magnetization vectors, $|\mathbf{M}_1| = |\mathbf{M}_2| = M_0$; $\mathbf{M} = \mathbf{M}_1 + \mathbf{M}_2$; z is the anisotropy axis, $\hat{N}$ is the tensor of demagnetizing factors; $2\pi \mathbf{M} \hat{N} \mathbf{M}$ is the energy of the demagnetizing field $\mathbf{H}_M = -4\pi \hat{N} \mathbf{M}$. Let us restrict our discussion of the energy of the demagnetizing field to a sample in the shape of an ellipsoid of rotation. The limiting shapes of an ellipsoid of rotation are a long cylinder and a plane-parallel plate, and the sphere is a particular case.

Assuming that the angle between $\mathbf{H}$ and the axis of the ellipsoid is small, we can neglect the off-diagonal components of the tensor $\hat{N}$. Then

$$\hat{N} = \begin{pmatrix} N_x & 0 & 0 \\ 0 & N_y & 0 \\ 0 & 0 & N_z \end{pmatrix}, \quad \mathrm{Sp}\, \hat{N} = 1.$$

If $\mathbf{H}$ lies in the zx plane and makes an angle ψ with the z axis, then $\mathbf{M}_1$ and $\mathbf{M}_2$ also lie in this plane. Then we can rewrite (1) in the form

$$\mathcal{H}/M_0 = -H_E \cos 2\theta - 2H \sin\theta \cos(\varphi - \psi) - (H_A/2)[\sin^2(\varphi+\theta) + \sin^2(\varphi-\theta)] - 8\pi M_0 k \sin^2\theta, \qquad (2)$$

where $k = N_z \cos^2\varphi + N_\perp \sin^2\varphi$, φ is the angle between the

antiferromagnetism vector $\mathbf{l} = \mathbf{M}_1 - \mathbf{M}_2$ and x, θ is the angle between $\mathbf{M}_1$ and $\mathbf{l}$ (or $\mathbf{M}_2$ and $-\mathbf{l}$), $N_x = N_y = N_\perp$, and ψ is the small angle between $\mathbf{H}$ and z (see the inset in Fig. 9).

By minimizing (2) with respect to φ and θ, we can obtain the following expressions relating θ, φ, ψ, and H:

$$\sin\theta = \frac{H\cos(\varphi-\psi)}{B}, \tag{3}$$

$$H^2 = \frac{B^2 H_A \sin 2\varphi}{B\sin 2(\varphi-\psi)+2\cos^2(\varphi-\psi)\sin 2\varphi[H_A-4\pi M_0(N_z-N_\perp)]}, \tag{4}$$

where

$$B=2H_E-H_A\cos 2\varphi+8\pi M_0 k.$$

Using expressions (3) and (4) for given values of H and ψ, we can find θ and, hence, the magnetization $\mathbf{M}$ under the condition that $H_A - 4\pi M_0(N_z - N_\perp) > 0$. Depending on the value of H, different AF states are realized. Assuming $\psi = 0$ and $\varphi = \pi/2$, we can use (4) to find the field boundary H_1 of the AF phase; for $\psi = 0$ and $\varphi = 0$ we find the field boundary H_2 of the SF phase:

$$H_1^2 = H_A(2H_{E1}+H_A),$$
$$\text{where } H_{E1} = H_E + 4\pi M_0 N_\perp, \tag{5}$$
$$H_2^2 = H_A\frac{(2H_{E2}-H_A)^2}{2H_{E1}+H_A},$$
$$H_{E2} = H_E + 4\pi M_0 N_z. \tag{6}$$

If $2H_{E1} + H_A > 2H_{E2} - H_A$, which is equivalent to the condition $H_A - 4\pi M_0(N_z - N_\perp) > 0$, then $H_1 > H_2$ and, consequently, the existence regions of the AF and SF phases overlap. In the overlap region the AF and SF phases are metastable. The energies of the phases become equal in a field

$$H_t = [(2H_{E2}-H_A)H_A]^{1/2}.$$

Figure 9 shows the $\varphi(H)$ curves obtained from (4) for different ψ with the following values of the constants: $H_E = 46.5$ T, $H_A = 0.92$ T, $N_z = 0.8$, $N_\perp = 0.1$. For $\psi < \psi_{cr}$ there exists a field region in which every field value corresponds to two values of φ. This field region is bounded by the lability fields H_1 and H_2 given by (5) and (6). For $\psi \geqslant \psi_{cr}$ the multivaluedness vanishes, and the rotation of the sublattices occurs smoothly. The point at which the $\varphi(H)$ curves intersect, denoted by the coordinates H^* and φ^* in Fig. 9, corresponds to the same magnetization of the antiferromagnet for different angles of inclination of the field with respect to the z axis, i.e.,

$$M(H^*\varphi^*,\ \psi) = \text{const}$$

for $\psi_{cr} \leqslant \psi < \pi/4$ and, consequently, in a field H^* the frequency-field curves should intersect for different angles of inclination greater than the critical angle ψ_{cr}. This is the same field that H_1 and H_2 tend toward as the angle of inclination approaches the critical value ψ_{cr}. The value of H^* is obtained from (4) upon substitution of $\varphi = \pi/4$:

$$H^* = (H_{E1}+H_{E2})(H_A/(2H_{E1}+H_A))^{1/2}. \tag{7}$$

The condition $\partial H/\partial\varphi = 0$ for $\varphi = \pi/4$ implies the following expression for the critical angle:

$$\operatorname{tg}(\pi/4-\psi_{cr}) = \frac{H_E - H_A + 6\pi M_0 N_z - 2\pi M_0 N_\perp}{H_E + 2\pi M_0(N_z+N_\perp)}. \tag{8}$$

Taking into account that $\psi_{cr} \ll \pi/4$, we obtain to high accuracy

$$\psi_{cr} = \frac{H_A - 4\pi M_0(N_z-N_\perp)}{2M_E + 4\pi(N_z+N_\perp)M_0}. \tag{9}$$

We see from expression (9) that ψ_{cr} depends strongly on the shape of the sample for an antiferromagnet in which H_A and $4\pi M_0$ are of the same order of magnitude. As the demagnetizing factor along the anisotropy axis decreases, the critical angle increases. For a thin plate

$$\psi_{cr} = (H_A - 4\pi M_0)/(2H_E + 4\pi M_0),$$

for a sphere

$$\psi_{cr} = H_A/(2H_E + 8/3\pi M_0).$$

The maximum critical angle corresponds to the case of a plate in which the anisotropy axis lies in the plane of the plate and the deviation of the field occurs in the plane perpendicular to the plane of the plate. In this case we have for MnF_2

$$\psi_{cr} = (H_A + 4\pi M_0)/(2H_E - 4\pi M_0) \approx 1°.$$

Up till now we have been discussing the phase transition in an antiferromagnet having a uniform distribution of $\mathbf{l}$ and $\mathbf{M}$ over the sample, but it is possible to have a nonuniform distribution of $\mathbf{l}$ and $\mathbf{M}$ as a result of the fact that in a certain field interval H_{t1}–H_{t2} it is energetically favorable for the sample to break up into domains of the AF and SF phases.

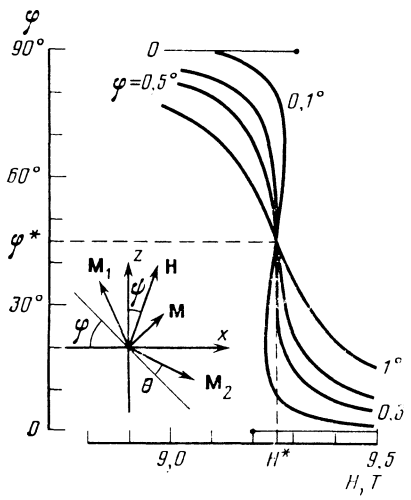

FIG. 9. Curves of $\varphi(H)$ for various ψ. The inset shows the relationship of $\mathbf{M}_1$, $\mathbf{M}_2$, and $\mathbf{H}$; z is the anisotropy axis.

This is just the intermediate state, whose energy is smaller than the energy of the AF and SF phases.[1] The dimensions of the domains and the thickness of the domain walls are determined by the values of the phenomenological constants and the dimensions of the sample. The transition field H_{t1} from the AF to the intermediate state depends only weakly on the shape of the sample and is given by[1]

$$H_{t1}=[(2H_E-H_A)H_A]^{1/2}+\Delta. \tag{10}$$

As H increases, the internal field in the interior of the sample in the intermediate state is uniform and remains unchanged and equal to H_{t1}.

At the field H_{t2} there is a transition from the intermediate state to the SF phase; here[1]

$$H_{t2}=H_{t1}+4\pi N_z|\mathbf{M}|-\Delta. \tag{11}$$

For a thin plate, Δ in (10) and (11) is a small quantity ($\Delta \ll 4\pi N_z M_z$) and in the majority of cases can be neglected. Consequently, the magnetic-field interval in which the intermediate state exists is given by

$$\Delta H_{IS}=H_{t2}-H_{t1}\approx 4\pi N_z M_z, \tag{12}$$

where $\mathbf{M}$ is the magnetization in the SF phase. Using (3) and taking into account that in the SF phase $|\mathbf{M}|=2M_0\sin\theta$ and $\varphi=0$, we have

$$\Delta H_{IS}=4\pi N_z|\mathbf{M}(H_{t2})|=\frac{8\pi N_z M_0}{2H_{E2}-H_A}H_{t2}\equiv\frac{8\pi N_z M_0}{2H_E-H_A}H_{t1}. \tag{13}$$

If we also take (10) into account, we get

$$\Delta H_{IS}=8\pi M_0 N_z H_A/H_{t1}. \tag{14}$$

Assuming that the critical angle for the metastable state is equal to the critical angle of the intermediate state, we find from (7), (9), (10), and (14) that

$$\psi_{cr}=\frac{4H_A^2-3(\Delta H_{IS})H_{t1}+8\pi M_0 H_A}{4(H_A^2+H_{t1}^2)+(\Delta H_{IS})H_{t1}+8\pi M_0 H_A}, \tag{15}$$

$$H^*=2^{-1/2}\frac{4H_{t1}^2+4H_A^2+(\Delta H_{IS})H_{t1}+8\pi M_0 H_A}{[2H_{t1}^2+4H_A^2-(\Delta H_{IS})H_{t1}+8\pi M_0 H_A]^{1/2}}. \tag{16}$$

If a plane-parallel plate is located in a field inclined to the z axis at an angle less than ψ_{cr}, the formation of the intermediate state is preceded by the smooth rotation of the sublattices, which continues until the formation of the domain structure becomes possible in a field $H_{t1}'>H_{t1}$. Here the domains of each of the phases will have a nonzero magnetization. At a field $H_{t2}'<H_{t2}$ there is a transition from the intermediate state to the SF phase, and a further increase in the field strength will change the magnetization on account of the rapid decrease of the angle φ. When the angle of inclination of the field approaches the value ψ_{cr} the difference between the domains of the coexisting phases decreases; the angle φ for each of the phases approaches $\pi/4$ and, consequently, the intermediate-state region contracts to a point. Because the energy of the domain walls decreases as $\psi\to\psi_{cr}$, the breakup into domains is favorable all the way to extremely small differences between the magnetizations of the coexisting phases and, consequently, formula (15) can be applied with good accuracy even for a sample in the intermediate state. A more rigorous expression for ψ_{cr} was obtained in Ref. 13.

The resonance modes in a uniaxial crystal are excited by a circularly polarized electromagnetic wave. If the wave is linearly polarized, it can be represented as the sum of two circularly polarized waves with right and left polarizations, which have different propagation velocities in an antiferromagnet in an external magnetic field, and, consequently, there is a rotation of the plane of polarization (the Faraday rotation) by an angle (see, e.g., Ref. 14):

$$\Phi=\pi\nu n_0\,\mathrm{Re}\,(\mu_+^{1/2}-\mu_-^{1/2})l, \tag{17}$$

where n_0 is the refractive index far from absorption lines, ν is the frequency, $\mu_\pm=1\pm 4\pi\chi_\pm$, $\chi_\pm$ is the susceptibility for right and left circularly polarized waves, and l is the thickness of the sample. Substituting into (17) the value of the susceptibility[14]

$$\chi_\pm=\frac{2\gamma^2 M_0 H_A}{(\omega_\pm-\omega)(\omega_\mp+\omega)},$$

where γ is the gyromagnetic ratio and $\omega=2\pi c\nu$, we obtain the following expression for the Faraday rotation angle of an antiferromagnet in a field $H\ll H_{t1}$ ($\mathbf{H}\|z$):

$$\Phi_{AF}=4\pi^2 n_0\nu(\gamma')^2 M_0 H_A\left[\frac{1}{(\nu_+-\nu)(\nu_-+\nu)}-\frac{1}{(\nu_--\nu)(\nu_++\nu)}\right]l, \tag{18}$$

where $\nu_\pm$ [cm^{-1}] are the resonance frequencies of the high-frequency and low-frequency modes, and $\gamma'=10^3\gamma/2\pi c=0.934$ ($\mathrm{cm}^{-1}/\mathrm{T}$). This formula is valid far from absorption lines. The dependence of Φ_{AF} on H is determined by the values of the frequencies $\nu_\pm$. At the transition field H_{t1} we have $\nu_-\approx 0$ and $\nu_+\approx 2\nu_0$, where ν_0 is the resonance frequency at $H=0$ and, consequently,

$$\Phi_{AF}\approx 16\pi^2 n_0(\gamma')^2 M_0 H_A\nu_0 l/(4\nu_0^2-\nu^2). \tag{19}$$

The Faraday rotation angle for an antiferromagnet in the SF state is given by an expression analogous to that obtained for a ferromagnet[13]:

$$\Phi_{SF}=-4\pi^2\gamma' n_0|\mathbf{M}|l. \tag{20}$$

We see from expressions (19) and (20) that the Faraday rotation angles near the intermediate state for the AF and SF phases are of opposite sign, and the total change in the angle is by an amount proportional to $|\mathbf{M}|$ (the frequencies $\nu_\pm$ are constant within the intermediate-state region). Because $|\mathbf{M}|$ changes linearly with increasing field in the intermediate state, the Faraday rotation angle should also vary linearly. If the analyzer is turned by an angle of $\pi/4$ with respect to the position corresponding to the maximum or minimum intensity of the electromagnetic wave transmitted through it, then, as we know, at a small Faraday rotation angle the intensity of this wave will be proportional to the angle itself. Consequently, the boundaries of the linear region on the oscilloscope trace of $I(H,\nu\approx\nu^*)$ when the analyzer is set at an angle of $\pi/4$ will correspond to the boundaries of the intermediate-state region. The frequency ν at which the measure-

ments are made is chosen approximately equal to ν^* in order to decrease the influence of the wings of the absorption lines whose maxima are found at the frequencies of the horizontal regions on the frequency-field curves (Fig. 4); these regions can distort the linear behavior of $I(H)$ in the intermediate-state region.

5. DISCUSSION

We have discussed some of the results in the previous sections. Here we shall focus on the experimental results shown in Figs. 3, 4, and 8. These results on the whole correspond to the ideas of the theory of the AFMR and the intermediate state which were briefly set forth in Sec. 4. For the intermediate-state region there is a good correlation among the AFMR, Faraday rotation, and χ_z data. Comparison of these data leads to the following conclusion: there is an interval of fields $\Delta H_{IS} = H_{t2} - H_{t1}$ within which the Faraday rotation angle varies linearly with the strength of the magnetic field, while the AFMR frequencies do not depend on H. Evidently, this interval should also be regarded as the existence region of the coherent intermediate state in the greater part of the sample. It follows from Figs. 4 and 8 that the field H_{t1} corresponds to the maximum of the susceptibility signal $\chi_z(H)$, while the field H_{t2} corresponds to the sharp change in $\chi_z(H)$ at the trailing edge. This indicates that the formation of a regular domain structure is preceded by an irregular and inhomogeneous distribution of the magnetization, wherein the local magnetizations are noncollinear with one another and with the direction of **H** and do not contribute to the Faraday rotation and AFMR in the intermediate state, although the total magnetization reaches an appreciable value. It should be noted that for a strict orientation of the magnetic field along the C_4 axis the field interval read off from the half-maximum of $\chi_z(H)$, often taken as the existence region of the intermediate state, actually is equal to the interval ΔH_{IS}, but shifted to lower fields.

The experimentally determined values $\psi_{cr} = 18 \pm 1'$, $H_{t1} = 9.2 \pm 0.01$ T, and $\Delta H_{IS} = 0.1 \pm 0.005$ T make it possible to find H_A and to estimate the effective demagnetizing factor. The constants H_E and H_A have been determined in several theoretical[15,16] and experimental[10,17] studies, where the values $H_E = 55$ T and $H_A = 0.86$ T were found. It must be noted, however, that those studies used initial data taken from results obtained in different experiments and on different samples. At the same time, however, a small (0.4%) admixture of iron,[18] for example, substantially alters the value of the transition field H_{t1} (from 9.25 to 9.6 T).

In our samples the value of H_{t1} agrees well with the values obtained previously,[4,18] although the previously obtained[3,4] value $\Delta H_{IS} = 0.09$ T is somewhat different from the one we measured, apparently because of a difference in the shape of the sample. Using only the experimental values of ψ_{cr}, H_{t1}, ΔH_{IS}, and $M_0 = 5.8 \cdot 10^{-2}$ T (Ref. 10), we find from (15) that $H_A = 0.91 \pm 0.02$ T; knowing this value, we use formulas (10) and (14) to get $H_E = 47 \pm 1.1$ T and $N_z = 0.7$. This value of the effective demagnetizing factor is in good agreement with the value 0.8 obtained for the axial demagnetizing factor N_z for an ellipsoid of rotation fitted to the actual shape of the sample.

Let us now turn our attention to the following circumstance. The frequency-field curve of the AFMR at $\psi = 0$ with allowance for the demagnetizing factor can be calculated with the formulas given in Ref. 19. The theoretical frequency-field curve of the SF mode with allowance for the values of H_A, H_E, and N_z obtained in the present study is given in Fig. 4. We see that this curve is substantially different from the experimental curve for the SF mode near the intermediate-state region. This behavior of the frequency-field curve could seemingly be explained by an inclination of the C_4 axis of the sample with respect to **H**. An estimate of the corresponding angle of inclination gives a value $\psi \approx 10'$. Such a large error in the orientation of the sample can be ruled out, since the high-frequency mode of the AFMR has a frequency deviation from the calculated value near the intermediate state of less than 0.2 cm^{-1}, which corresponds to an angle of inclination of less than 3'. All of the samples which we studied gave approximately the same results. The only difference lay in the rise time of $\chi_z(H)$ and the value of the low-frequency wing of the absorption line of the high-frequency mode (in a frequency cross section) in the intermediate-state region; here there was agreement between these features: a more protracted leading edge of $\chi_z(H)$ corresponded to a more diffuse absorption line in the intermediate-state region. Using a thicker sample and cementing the thin sample to the substrate produced similar behavior. Obviously, the rise time of the susceptibility depends on the quality of the sample, its shape, and the uniformity of the external magnetic field, i.e., in the final analysis, on the uniformity of the internal field. The internal field is most strongly distorted near the corners and edges of the sample and remains fairly uniform in the interior of the sample. It must also be noted that the sample itself can be inhomogeneous. For example, there can be individual large blocks or a large number of small blocks with a random distribution of their anisotropy axes within a small angle. It is not hard to see that these defects would give rise to significant deviation of the frequency-field curve for the high-frequency mode or to the appearance of additional absorption lines near the horizontal regions. Thus, the experimental data show that the samples we investigated were of high quality and their orientation was quite accurate, and, consequently, the deviation present in the frequency-field curve of the SF mode near the intermediate-state region from the theoretical curve cannot be explained solely by these causes. The deviation of the experimental frequency-field curve from the calculated curve for the SF mode near the intermediate-state region might be due to anisotropy in the basal plane, which was recently detected[20] in MnF_2, but estimates of the influence of fourth-order anisotropy on the behavior of the resonance modes in the region of the SF transition in samples of finite dimensions will require an appropriate theoretical treatment.

6. CONCLUSIONS

We have studied the behavior of the AFMR in the region of the intermediate state, which has the following char-

acteristics: 1) the frequencies are independent of the strength of the external magnetic field, i.e., there are horizontal regions on the frequency-field curve, with lengths equal to the width of the intermediate-state region; these regions shift and contract as the field deviates from the ordering axis; 2) there are "windows" of transparency in the frequency-field curve for a strict orientation of the field along the C_4 axis; these windows vanish when the angle of inclination reaches a critical value ψ_{cr}; 3) the resonance lines have a characteristic shape during a field sweep at the frequencies of the horizontal region with an approximately linear fall-off in the intermediate-state region and with a Lorentzian character outside the intermediate state; 4) the lines are broadened. All these characteristics indicate that the internal magnetic field is constant and uniform in the greater part of the sample in the intermediate state, that there is no dynamic coupling between the oscillations in the domains of the AF and SF phases, that the intensity of the lines is proportional to the fraction of the material in the corresponding phase, and also that inhomogeneities in the form of domain walls appear.

The joint experimental study of the AFMR, Faraday effect, and static magnetic susceptibility has shown that the existence region of the coherent intermediate state should be taken to be the field interval within which the AFMR frequency remains unchanged and the Faraday rotation angle changes linearly with the field. The beginning of this region corresponds to the maximum of $\chi_z(H)$, and the end corresponds to the sharp change on the trailing edge of $\chi_z(H)$. The size of the transparency window on the frequency-field curve at $\psi = 0$ is determined by the quality of the sample; this raises the possibility of monitoring the quality of a sample down to a determination of the volume of the blocks and the angular misalignment of their anisotropy axes.

[1]V. G. Bar'yakhtar, A. E. Borovik, and V. A. Popov, Pis'ma Zh. Eksp. Teor. Fiz. **9**, 634 (1969) [JETP Lett. **9**, 391 (1969)]; Zh. Eksp. Teor. Fiz. **62**, 2233 (1972) [Sov. Phys. JETP. **35**, 1169 (1972)].

[2]K. L. Dudko, V. V. Eremenko, and V. M. Fridman, Zh. Eksp. Teor. Fiz. **61**, 678, 1553 (1971) [Sov. Phys. JETP **34**, 362, 828 (1972)].

[3]A. A. Mil'ner, Yu. A. Popkov, and V. V. Eremenko, Pis'ma Zh. Eksp. Teor. Fiz. **18**, 39 (1973) [JETP Lett. **18**, 20 (1973)].

[4]A. R. King and D. Paquette, Phys. Rev. Lett. **30**, 662 (1973).

[5]V. G. Bar'yakhtar, A. A. Galkin, S. N. Kovner, and V. A. Popov. Zh. Eksp. Teor. Fiz. **58**, 494 (1970) [Sov. Phys. JETP **31**, 264 (1970)]; A. A. Galkin, S. N. Kovner, and V. A. Popov, Phys. Status Solidi B **57**, 485 (1973).

[6]A. I. Mitsek, P. F. Gaidanskii, and V. N. Pushkar, Phys. Status Solidi **38**, 69 (1970).

[7]A. N. Bogdanov and V. T. Telepa, Preprint No. 38 [in Russian], Physicotechnical Institute, Donetsk (1982).

[8]V. V. Eremenko, A. V. Klochko, and V. M. Naumenko, Pis'ma Zh. Eksp. Teor. Fiz. **35**, 479 (1982) [JETP Lett. **35**, 591 (1982)].

[9]V. M. Naumenko, V. V. Eremenko, and A. V. Klochko, Prib. Tekh. Eksp. **4**, 159 (1981).

[10]F. M. Johnson and A. N. Nethercot Jr., Phys. Rev. **114**, 705 (1959).

[11]E. A. Turov, Fizicheskie Svoĭstva Magnitouporyadochennykh Kristallov, Izd. AN SSSR, Moscow (1963) [Physical Properties of Magnetically Ordered Crystals, Academic Press, New York (1965)].

[12]V. A. Popov and V. I. Skidanenko, Fizika Kondensirovannogo Sostoyaniya [Physics of the Condensed State], Vyp. VII, Physicotechnical Institute of Low Temperatures, Academy of Sciences of the Ukrainian SSR, Kharkov (1970), p. 49.

[13]V. G. Bar'yakhtar, A. P. Bogdanov, V. T. Telepa, and D. A. Yablonskiĭ, Proc. All-Union Seminar on Magnetic Phase Transitions and Critical Phenomena [in Russian], Makhachkala (1984), p. 28.

[14]A. G. Gurevich, Magnitnyi Rezonans v Ferritakh i Antiferromagnetikakh [Magnetic Resonance in Ferrites and Antiferromagnets], Nauka, Moscow (1973), pp. 170, 240.

[15]T. Oguchi, Phys. Rev. **111**, 1063 (1958).

[16]F. Keffer, Phys. Rev. **87**, 608 (1952).

[17]R. W. Sanders, R. M. Belanger, M. Motokawa, and V. Jaccarino, Phys. Rev. B **23**, 1190 (1981).

[18]R. Blewit and R. Weber, J. Appl. Phys. **41**, 884 (1970).

[19]V. A. Popov and V. I. Skidanenko, Preprint [in Russian], Physicotechnical Institute of Low Temperatures, Academy of Sciences of the Ukrainian SSR, Kharkov (1972).

[20]V. V. Eremenko, N. É. Kaner, Yu. G. Litvinenko, A. A. Mil'ner, V. V. Shapiro, Fiz. Nizk. Temp. **11**, 62 (1985) [Sov. J. Low Temp. Phys. **11**, (1985)].

Translated by Steve Torstveit